

## Retrospective Cohort Study

# Visualizing the hepatic vascular architecture using superb microvascular imaging in patients with hepatitis C virus: A novel technique

Hidekatsu Kuroda, Tamami Abe, Keisuke Kakisaka, Yudai Fujiwara, Yuichi Yoshida, Akio Miyasaka, Kazuyuki Ishida, Hideaki Ishida, Tamotsu Sugai, Yasuhiro Takikawa

Hidekatsu Kuroda, Tamami Abe, Keisuke Kakisaka, Yudai Fujiwara, Yuichi Yoshida, Akio Miyasaka, Yasuhiro Takikawa, Division of Hepatology, Department of Internal Medicine, Iwate Medical University, School of Medicine, Morioka, Iwate 020-8505, Japan

Kazuyuki Ishida, Tamotsu Sugai, Department of Molecular Diagnostic Pathology, Iwate Medical University, Morioka, Iwate 020-8505, Japan

Hideaki Ishida, Center of Diagnostic Ultrasound, Akita Red Cross Hospital, Akita 010-1495, Japan

University, School of Medicine, Uchimarui9-1, Morioka, Iwate 020-8505, Japan. [hikuro@iwate-med.ac.jp](mailto:hikuro@iwate-med.ac.jp)  
Telephone: +81-19-6515111  
Fax: +81-19-6526664

Received: March 2, 2016  
Peer-review started: March 3, 2016  
First decision: April 1, 2016  
Revised: April 5, 2016  
Accepted: April 20, 2016  
Article in press: April 20, 2016  
Published online: July 14, 2016

**Author contributions:** All the authors contributed to this paper.

**Institutional review board statement:** The study was reviewed and approved for publication by our Institutional Reviewer.

**Informed consent statement:** All study participants or their legal guardian provided informed written consent about personal and medical data collection prior to study enrollment.

**Conflict-of-interest statement:** All the Authors have no conflict of interest related to the manuscript.

**Data sharing statement:** The original anonymous dataset is available on request from the corresponding author at [hikuro@iwate-med.ac.jp](mailto:hikuro@iwate-med.ac.jp).

**Open-Access:** This article is an open-access article which was selected by an in-house editor and fully peer-reviewed by external reviewers. It is distributed in accordance with the Creative Commons Attribution Non Commercial (CC BY-NC 4.0) license, which permits others to distribute, remix, adapt, build upon this work non-commercially, and license their derivative works on different terms, provided the original work is properly cited and the use is non-commercial. See: <http://creativecommons.org/licenses/by-nc/4.0/>

**Correspondence to:** Hidekatsu Kuroda, MD, PhD, Division of Hepatology, Department of Internal Medicine, Iwate Medical

## Abstract

**AIM:** To identify the hepatic vascular architecture of patients with hepatitis C virus (HCV) using superb microvascular imaging (SMI) and investigate the use of SMI in the evaluation of liver fibrosis.

**METHODS:** SMI was performed in 100 HCV patients. SMI images were classified into five types according to the vascular pattern, and these patterns were compared with the fibrosis stage. Moreover, the images were analyzed to examine vascularity by integrating the number of SMI signals in the region of interest ROI [number of vascular trees (VT)]. The number of VT, fibrosis stage, serum parameters of liver function, and CD34 expression were investigated.

**RESULTS:** There was a significant difference between SMI distribution pattern and fibrosis stage ( $P < 0.001$ ). The mean VT values in each of the fibrosis stages were as follows:  $26.69 \pm 7.08$  in F0,  $27.72 \pm 9.32$  in F1,  $36.74 \pm 9.23$  in F2,  $37.36 \pm 5.32$  in F3, and  $58.14 \pm 14.08$  in F4. The VT showed excellent diagnostic ability for F4 [area under the receiver operator characteristic

(AUROC): 0.911]. The VT was significantly correlated with the CD34 labeling index ( $r = 0.617$ ,  $P < 0.0001$ ).

**CONCLUSION:** SMI permitted the detailed delineation of the vascular architecture in chronic liver disease. SMI appears to be a reliable tool for noninvasively detecting significant fibrosis or cirrhosis in HCV patients.

**Key words:** Superb microvascular imaging; Number of vascular trees; Chronic liver disease; Ultrasound; Liver fibrosis; CD34

© **The Author(s) 2016.** Published by Baishideng Publishing Group Inc. All rights reserved.

**Core tip:** Superb microvascular imaging (SMI) is an innovative Doppler ultrasound technology that employs a unique algorithm to allow for the visualization of minute vessels with slow blood flow. In the present study, we identified the hepatic vascular architecture of patients with hepatitis C virus (HCV) using SMI and investigated the use of SMI in the evaluation of liver fibrosis. SMI allowed for the detailed delineation of the vascular architecture in chronic liver disease patients. Significant differences were found in the SMI pattern distribution and the fibrosis stage. SMI appears to be a reliable tool for noninvasively detecting significant fibrosis or cirrhosis in patients with HCV.

Kuroda H, Abe T, Kakisaka K, Fujiwara Y, Yoshida Y, Miyasaka A, Ishida K, Ishida H, Sugai T, Takikawa Y. Visualizing the hepatic vascular architecture using superb microvascular imaging in patients with hepatitis C virus: A novel technique. *World J Gastroenterol* 2016; 22(26): 6057-6064 Available from: URL: <http://www.wjgnet.com/1007-9327/full/v22/i26/6057.htm> DOI: <http://dx.doi.org/10.3748/wjg.v22.i26.6057>

## INTRODUCTION

Hepatitis C virus (HCV) has a high propensity to persist and cause chronic hepatitis, eventually leading to cirrhosis<sup>[1-3]</sup>. Cirrhosis results from different mechanisms of liver injury, which lead to hepatic necroinflammation and fibrogenesis. It is histologically characterized by diffuse nodular regeneration surrounded by dense fibrotic septa with subsequent parenchymal extinction and the collapse of liver structures<sup>[4]</sup>. Together, these effects cause the pronounced distortion of the hepatic vascular architecture, which results in increased resistance to the portal blood flow and, consequently, portal hypertension and hepatic synthetic dysfunction. The distortion of the hepatic vascular architecture is, therefore, a major determinant of hepatic repair and the regenerative capability<sup>[5,6]</sup>. Furthermore, the evaluation of the hepatic vascular architecture is useful for assessing the chronic liver disease (CLD) state, determining treatment strategies, and elucidating the mechanisms of disease progression.

Several studies using hepatic angiography have reported that vascular tortuosity, tapering, unevenness of branching and grouping of branches are associated with the progression of CLD<sup>[7-12]</sup>; however, angiography is an invasive medical test. Recent research has, therefore, focused on the evaluation of noninvasive methods to identify valid, flexible, and accurate methods for assessing the distortion of the hepatic vascular architecture. The ultrasound Doppler technique, a noninvasive, radiation-free technique, is widely used to observe hepatic blood flow and vascular architecture. However, there are some technical limitations associated with this technique, such as visualization of the fine vessels and low velocity blood flow<sup>[13,14]</sup>. Contrast-enhanced ultrasound (CEUS) detects low velocity blood flow in the microcirculation and is thus able to overcome some of these limitations. However, it does have a number of drawbacks: it is not readily available, it is subject to certain restrictions regarding contrast agent use, and it places an additional cost burden on the patient.

In recent years, Toshiba Medical Systems has developed a new Doppler technique called superb microvascular imaging (SMI)<sup>[15,16]</sup>. SMI is a microvascular flow imaging mode that is designed to improve blood flow visualization, especially slow flow signals from microscopic vessels, using a new adaptive algorithm that dramatically removes clutter while maintaining very high frame rates. In the present study, we identified the hepatic vascular architecture of patients with HCV-related CLD using SMI and investigated the use of SMI in the evaluation of liver fibrosis.

## MATERIALS AND METHODS

### Patients

One hundred nineteen patients with HCV-related CLD who had undergone a liver biopsy at our institution between January and November 2015 were involved in this study. HCV-related CLD was diagnosed according to the results of a histological analysis and the detection of HCV antibodies in the serum using a third-generation enzyme-linked immunosorbent assay (Abbott Labs, Abbott Park, IL, United States). Patients with a history of drug and/or alcohol abuse (alcohol consumption of  $\geq 40$  g/d for men,  $n = 3$ ,  $\geq 20$  g/d for women over past 12 mo,  $n = 3$ ), hepatitis B surface antigen positivity ( $n = 2$ ), severe obesity [body mass index (BMI)  $> 30$  kg/m<sup>2</sup>,  $n = 4$ ], severe fatty liver ( $n = 4$ ), and other CLD, such as primary biliary cirrhosis and autoimmune hepatitis ( $n = 3$ ), were excluded from the present study. Among these patients, 19 patients were excluded from the analysis. Finally, data were obtained from a total of 100 patients. The mean ( $\pm$  SD) age of the patients was  $65.8 \pm 10.4$  years (range: 41-85 years). The subjects included 56 men and 44 women. The patient profiles are presented in Table 1. The study was approved by the local Ethical Committee of Iwate Medical University (H26-124). The

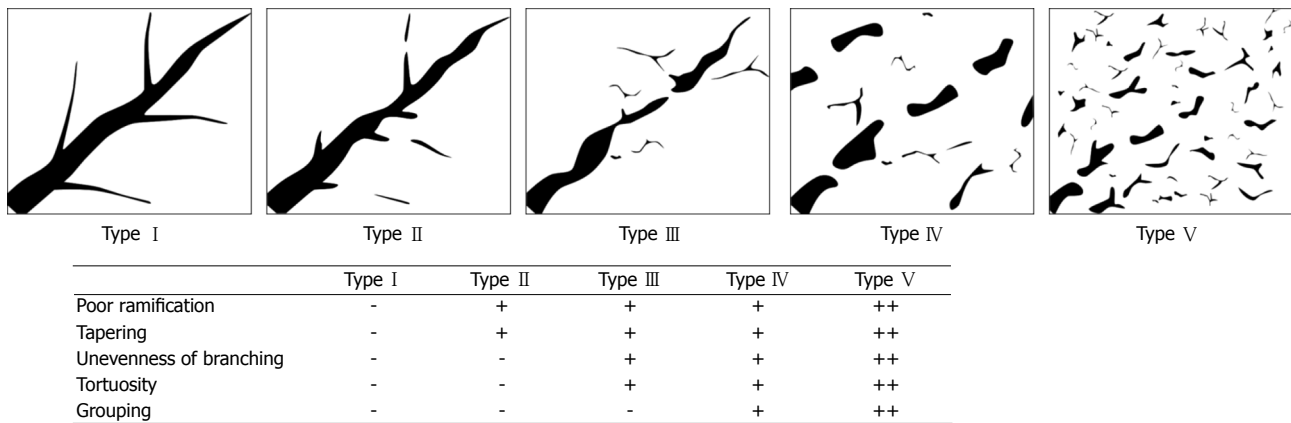


**Figure 1 Superb microvascular imaging vascular patterns.** Type I, clearly defined vessels with no irregularities; Type II, poor ramification and tapering of the main branches; Type III, mild tortuosity of the main branches and uneven branching; Type IV, moderate tortuosity and mild grouping of the main branches; and Type V, severe tortuosity and grouping of the main branches.

**Table 1 Baseline characteristics of patients**

Variables	n = 100
Sex (male/female)	56/44
Mean age (yr)	65.8 ± 10.5
BMI (kg/m <sup>2</sup> )	22.8 ± 3.3
METAVIR score (F0/F1/F2/F3/F4)	21/34/11/11/23
T-Bil (mg/dL)	0.6 (0.5-0.8)
AST (U/L)	35.5 (25.8-53.1)
ALT (U/L)	32.6 (23.6-53.8)
Alb (g/dL)	3.9 (3.5-4.2)
PT (%)	92.1 (82.2-98.8)
Plt (× 10 <sup>4</sup> /mm <sup>3</sup> )	14.8 (11.3-18.2)
HA (ng/mL)	101 (92.1-117.5)
IV-c-7S (ng/mL)	5.7 (4.4-7.8)

The values represent the mean ± standard deviation or the median (25<sup>th</sup>-75<sup>th</sup> percentile). BMI: Body mass index; T-Bil: Total bilirubin; AST: Aspartate aminotransferase; ALT: Alanine aminotransferase; Alb: Albumin; PT: Prothrombin time; Plt: Platelet count; HA: Hyaluronic acid; IV-c-7S: Type IV collagen 7S.

patients provided their written informed consent before beginning the study in accordance with the principles of the Declaration of Helsinki (revision of Fortaleza, 2013).

#### Ultrasound examination technique

The ultrasound scanner Aplio500 (Toshiba Medical Systems, Otawara, Japan) combined with a 7.0 MHz linear transducer (PLT-705BT) was used. B-mode ultrasonography was performed to scan the whole liver before the SMI examination. The vascular architecture of the anterior-inferior portal vein was evaluated on monochrome SMI on the same day the patients underwent a liver biopsy. The anterior-inferior portal vein was selected because trans-abdominal ultrasound can provide a stable and high-resolution image. SMI was performed in the stable transducer position. The following settings were used for the SMI examination in all cases: the region of interest (ROI) was set to a fixed depth of 15 mm from the liver surface and the size of the ROI measured 40 mm ×

25 mm. The color velocity scale of SMI was adjusted to 1.4 to 1.6 cm/s, the color frequency was adjusted to 4 MHz, and the vascular information was enhanced by adjusting the time smooth. To avoid interobserver variability, all sonographic scanning was performed by two radiologists with > 10 years of experience in abdominal sonography and 3 mo of experience in SMI. A third radiologist with > 15 years of experience in abdominal sonography and 6 mo of experience in SMI served as a blinded expert in cases of disagreement.

According to previous hepatic angiographic reports regarding changes in vascular morphology that occur in CLD<sup>[7-12]</sup>, we classified portal vein vascular patterns into the five following types: Type I, clearly defined vessels with no irregularities; Type II, poor ramification and tapering of the main branches; Type III, mild tortuosity of the main branches and unevenness of branching; Type IV, moderate tortuosity and mild grouping of the main branches; and Type V, severe tortuosity and grouping of the main branches (Figure 1). Two additional radiologists who did not perform SMI blindly classified each of the SMI images as one of the five types according to the vascular pattern, and the frequencies of each pattern were compared with the fibrosis stages. At the end of the classification, any disagreement was discussed and resolved by a consensus.

The terminal branch of the anterior-inferior portal vein was scanned with SMI, and the maximum vessel lumen was selected for study. Flash or movement artifacts were excluded by repeated pulsed Doppler sampling of visible color signals to ensure that these signals originated from the portal veins. The images were recorded in the DICOM file format. The number of SMI vascular signals in the ROI was counted using an image analysis software program (ImageJ, National Institutes of Health, Bethesda, MD, United States)<sup>[17]</sup>. In the present study, we referred to the number of vascular signals as vascular trees (VT). The relationships between the VT and sex, age, BMI and the results of liver function tests were examined.

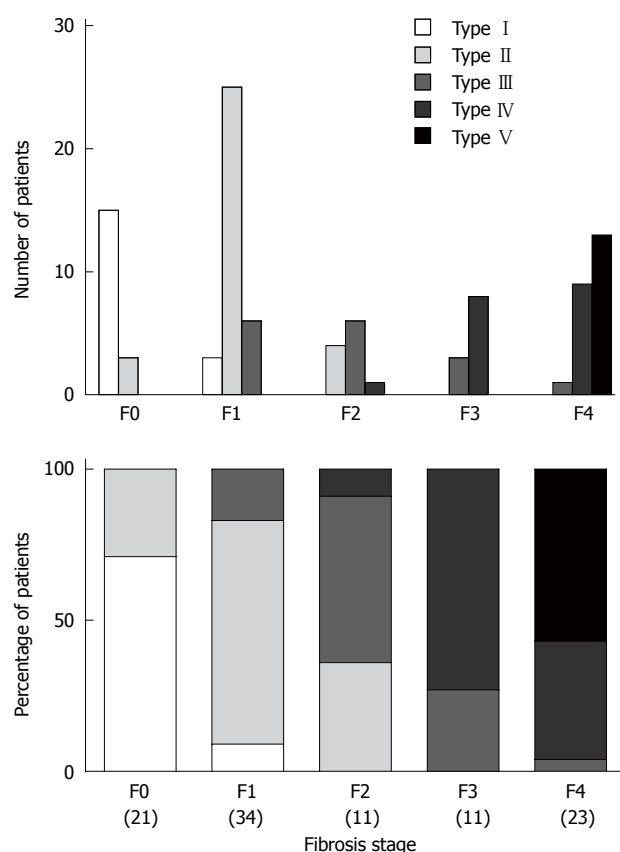


**Figure 2** Distribution of the superb microvascular imaging patterns and fibrosis stages. Fisher's exact probability test demonstrated a significant difference in the SMI pattern distribution and the fibrosis stage ( $P < 0.001$ ). SMI: Superb microvascular imaging.

### Serum markers of the liver function

Biochemical tests were performed in all patients on the day of SMI using routine laboratory methods. The tests included total bilirubin (T-Bil), albumin (Alb), aspartate aminotransferase (AST), alanine aminotransferase (ALT), prothrombin time (PT), platelet count (Plt), hyaluronic acid (HA), and type IV collagen 7S (IV-c-7S).

### Histology and immunohistochemistry

An echo-assisted liver biopsy was performed in the same session as SMI using a 14-G biopsy needle measuring 2.2 mm in diameter. The tissue specimens were immediately fixed in 10% buffered formalin, embedded in paraffin, and cut into 4 mm thick sections. These sections were stained with hematoxylin and eosin and Gomori trichrome stain and were assessed (according to the METAVIR score<sup>[18]</sup>) by two highly experienced pathologists who were blinded to the results of SMI and to all of the patients' clinical, serological, and histological data. All of the liver biopsy specimens were obtained from the pathology samples at Iwate Medical University Hospital. Fibrosis was staged on a 0-4 scale: F0, no fibrosis; F1, portal fibrosis without septa; F2, portal fibrosis and a small number of septa extending into the lobules; F3, numerous septa extending to the adjacent portal tracts

or terminal hepatic venules; and F4, cirrhosis.

CD34 is a 110 kDa transmembrane glycoprotein that is present on leukemic cells, endothelial cells and stem cells. CD34 is preferentially expressed on the surface of regenerating or migrating endothelial cells and is a marker of the proliferation of endothelial cells in growth during angiogenesis<sup>[19]</sup>. Normal sinusoidal endothelial cells do not typically express CD34. However, pathological conditions can alter their phenotype and cause them to express this marker. The capillarization of the hepatic sinusoids is a well-recognized phenomenon that occurs in CLD and hepatocellular carcinoma<sup>[20]</sup>. We performed immunohistochemical examinations to detect CD34 positivity in 61 of the patients in the present study. An anti-CD34 monoclonal mouse antibody (QEnd 10; Dako A/S, Glostrup, Denmark) was used. The avidin-biotin-peroxidase complex immunohistochemistry method (Vectastain Elite ABC Kit, Vector Laboratories Inc., Burlingame, CA, United States) was used. The number of CD34-positive capillaries and sinusoids were counted in 10 portal areas under a high-power field (200 × magnification) by two independent observers with no knowledge of the patient data. The average number was defined as the CD34 labeling index (CD34 LI). There was no significant interobserver difference; a few cases with wide differences were re-evaluated by a third observer. The present study evaluated the relationships among the fibrosis stage, the CD34 LI, and the number of VT.

### Statistical analysis

Statistical tests were performed using the SPSS 12.0 software program (SPSS, Chicago, IL, United States). The values are shown as the mean ± SD, or medians (range) according to the distribution of the values. Categorical data were compared using Fisher's exact probability test. A statistical analysis of the differences in the number of VT in each fibrosis stage was performed using the Kruskal-Wallis test. The correlations between the number of VT and other parameters were assessed using Spearman's rank correlation coefficient. The clinical diagnostic ability of the VT for cirrhosis was evaluated according to the sensitivity, specificity, and area under the receiver operating characteristic (AUROC) curve.  $P$  values of  $< 0.05$  were considered to indicate statistical significance.

## RESULTS

The average time required for the SMI examination was  $60.5 \pm 20.1$  s, and all patients cooperated with the examination. The association between the SMI pattern and fibrosis stage is presented in Figure 2. There was a significant difference in the distribution of the SMI pattern and the fibrosis stage ( $P < 0.001$ ). The percentage of patients with advanced fibrosis (F3-4) in SMI patterns I, II, III, IV, and V was 0% (0/18), 0% (0/35), 25% (4/16), 94% (17/18), and



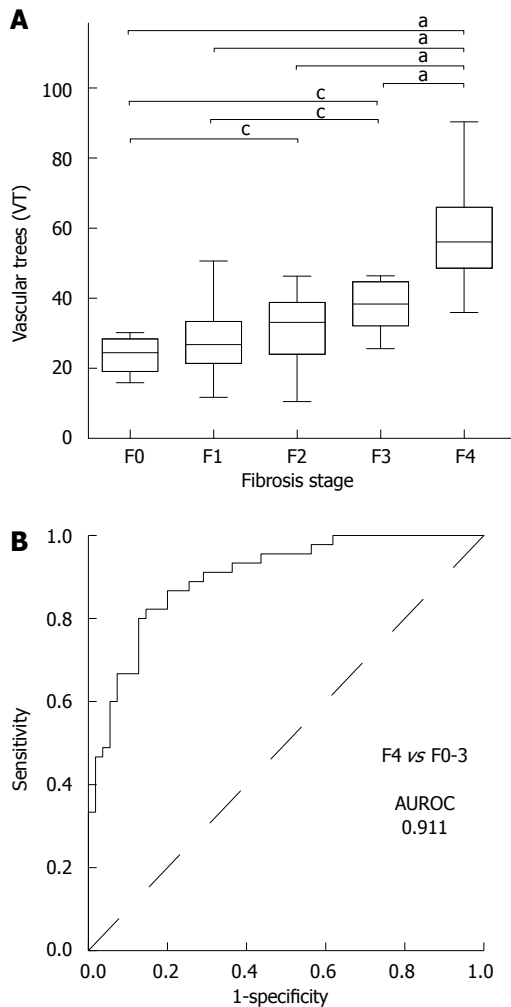


**Figure 3** Vascular tree values for the different fibrosis stages in patients who underwent liver biopsy (A) and the receiver operating characteristic curve of the vascular tree for the prediction of F4 in all 100 patients. The VT values increased in proportion to the fibrosis stage ( $^aP < 0.001$ ,  $^cP < 0.01$  by Kruskal-Wallis analysis). AUROC: Area under the receiver operating characteristic; VT: Vascular trees.

100% (13/13), respectively. Conversely, mild fibrosis (F0-1) occurred in 100% (18/18), 89% (31/35), 38% (6/16), 0% (0/18), and 0% (0/13) of patients, respectively.

The mean VT values in each of the fibrosis stages were as follows:  $26.69 \pm 7.08$  in F0 (21),  $27.72 \pm 9.32$  in F1 (34),  $36.74 \pm 9.23$  in F2 (11),  $37.36 \pm 5.32$  in F3 (11), and  $58.14 \pm 14.08$  in F4 (23). The mean VT value in F4 was significantly higher than those in F0-3 ( $P < 0.001$ ), while the mean values in F2 and F3 were higher than those in F0 and F1 ( $P < 0.01$ ) (Figure 3A). The ROC curve for the diagnosis of the F4 stage is shown in Figure 3B. The AUROC curve for the VT was 0.911. The most appropriate VT cut-off value for the diagnosis of F4 was 35.65, and the sensitivity and specificity were 82.2% and 85.5%, respectively.

The relationships between the VT and the clinical or laboratory parameters of the patients are shown in Table 2. The VT showed a significant negative

**Table 2** Correlation between the vascular trees values and clinical or laboratory parameters

Parameters	<i>r</i> value	<i>P</i> value
Sex	0.027	0.895
Age	0.213	0.073
BMI	-0.021	0.836
T-Bil.	0.079	0.435
AST	0.266	0.007
ALT	0.135	0.181
Alb	-0.498	< 0.001
PT	-0.435	< 0.001
Plt	-0.472	< 0.001
HA	0.567	< 0.001
IV-c-7S	0.428	< 0.001

VT: Vascular trees; BMI: Body mass index; T-Bil: Total bilirubin; AST: Aspartate aminotransferase; ALT: Alanine aminotransferase; Alb: Albumin; PT: Prothrombin time; Plt: Platelet count; HA: Hyaluronic acid; IV-c-7S: Type IV collagen 7S.

correlation with Plt, Alb, and PT ( $P < 0.01$ ) and a significant positive correlation with AST, HA, and IV-c-7S ( $P < 0.01$ ). The SMI images and the CD34 expression at different stages of fibrosis are presented in Figure 4. The CD34 expression was mainly confined to the small vessels in the portal area and was also seen in the sinusoids in the liver parenchyma near the portal areas, with dotted, linear, semicircular, and circular staining patterns. In the mild fibrosis group (F0-1), CD34 staining was restricted to the endothelium of portal vessels. In contrast, numerous CD34-labeled vessels were detected in the advanced fibrosis group (F3-4). The VT significantly correlated with the CD34 LI ( $r = 0.617$ ,  $P < 0.001$ ) (Figure 5).

## DISCUSSION

Doppler ultrasound is used to noninvasively measure blood flow velocity. To obtain high quality Doppler images, it is important to sufficiently suppress the clutter signals that originate from stationary and slowly moving tissue. The clutter signals overlap with the low velocity blood flow components. Clutter rejection filters are commonly used to remove the low frequency components in conventional Doppler imaging; however, these filters also cause the loss of signal from low velocity blood flow<sup>[13,14]</sup>. SMI is an innovative ultrasound Doppler technique. It analyzes the clutter motion and uses a new adaptive algorithm to identify and remove tissue motion, revealing the true blood flow. SMI also features high frame rates ( $> 50$  FPS) and high resolution. SMI operates in two modes: monochrome SMI (mSMI), which subtracts the background image from the detailed vasculature, and color SMI (cSMI), which displays the flow components in color overlaid on the grayscale B-mode image. SMI helps clinicians to visualize very small vascular structures and observe small branching details that previously were not visible. SMI

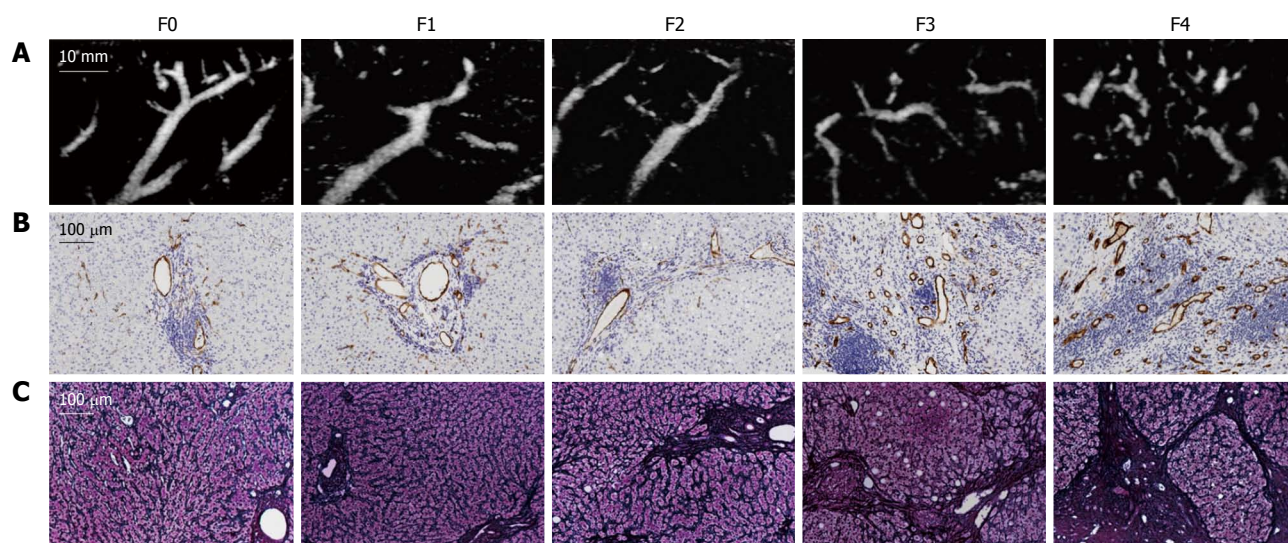


**Figure 4** Superb microvascular imaging images and CD34 expressions at different fibrosis stages. A: SMI image; B: CD34 expression; C: Gomori trichrome staining. SMI: superb microvascular imaging.

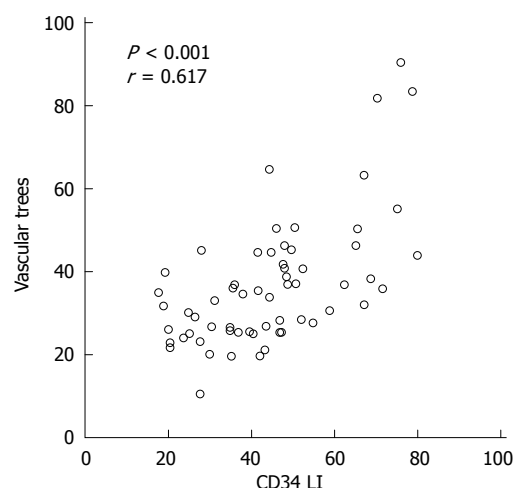


**Figure 5** Correlation between the vascular trees value and the CD34 labeling index. Spearman's rank correlation coefficient. LI: Labeling index.

does not use intravenous contrast agents, which is a significant advantage for patients who are often fearful of needles and injections. Recently, several clinical studies have reported the use of SMI technology in performing microvascular evaluations. Ma *et al.*<sup>[15]</sup> reported that SMI was more sensitive than color Doppler flow imaging for revealing the microvascular blood flow and vascularization of malignant breast tumors. According to their study, the detection of small vessels improved with the use of SMI compared with conventional Doppler ultrasound in malignant breast tumors. Moreover, Machado *et al.*<sup>[16]</sup> reported that SMI consistently improved the depiction of thyroid microvascular flow in comparison to standard color and power Doppler imaging. To the best of our knowledge, the present study provides the first comparison of the vascular pattern on SMI and fibrosis staging in CLD patients.

The present study demonstrated a significant difference in the distribution of the SMI pattern and fibrosis stage, and the number of VT was significantly higher in the F4 stage than in the other stages. In addition, the AUROC curve for early prediction of the F4 stage by the VT was 0.911, indicating its high accuracy. The mechanism underlying the increase in the VT is thought to be derived from the combination of vessel branch grouping through the fibrous expansion of portal areas, angiogenesis that occurs with chronic liver damage, and fragmentation of the vessels that is caused by severe tortuosity. Sugimoto *et al.*<sup>[21]</sup> reported such vascular tortuosity in advanced hepatic disease patients using CEUS. In fact, CEUS increases the detection of fine slow-velocity blood flow. However, the short arterial phase of the CEUS liver scan was not suitable for the present study.

An accurate evaluation of fibrosis in liver tissues is crucial for the differential diagnosis of CLD. A liver biopsy remains the reference standard for assessing liver fibrosis<sup>[22,23]</sup>. However, this procedure is invasive and it is associated with patient discomfort, sampling error and, in rare cases, serious complications. Recent research has thus focused on the evaluation of noninvasive, valid, accurate, and flexible methods of assessing liver fibrosis. In recent years, transient elastography, acoustic radiation force impulse imaging, and shear wave elastography have been reported to indicate reliably the stage of liver fibrosis<sup>[24-26]</sup>. However, ultrasonographic devices with these software programs are expensive high-end systems. In contrast, SMI is a noninvasive method that does not involve complicated operations and provides information that is superior to that obtained by color and power Doppler imaging. The results of this study indicate that SMI may be used for the early detection of advanced fibrosis.

The present study has shown that the VT is significantly correlated with PIt, AST, Alb, PT, HA, IV-c-7S, and the CD34 LI. In the present study, we performed an immunohistochemical analysis to evaluate the number of CD34-positive vessels. CD34 is preferentially expressed on the surface of regenerating or migrating endothelial cells and is a marker of proliferating endothelial cells in growth during angiogenesis. Our study is the first to show the number of SMI vascular signals to be correlated significantly with the CD34 expression.

There are several limitations associated with the present study. First, the study included a relatively small number of patients. A larger scale prospective clinical study is needed to quantify more accurately the optimal threshold of SMI for the diagnosis of fibrosis. Second, SMI is difficult to perform in obese individuals or patients with severe fatty liver due to the depth of subcutaneous fat; the increased distance between the deeper organs and the probe has a negative effect on the clarity of images of the hepatic vessels. Finally, the VT may depend on vessel fragmentation that occurs due to severe tortuosity. A method that allows for the three-dimensional examination of the hepatic vascular architecture is still needed.

In conclusion, SMI allowed the detailed delineation of the vascular architecture in CLD patients. Significant differences were found in the SMI pattern distribution and the fibrosis stage. The VT was significantly correlated with the expression of CD34. Thus, SMI appears to be a reliable tool for noninvasively detecting significant fibrosis or cirrhosis in patients with HCV. We now expect this imaging modality to continue to make further advances, including the development of three-dimensional SMI.

## ACKNOWLEDGMENTS

The authors thank Ms. Yuriko Mikami, Ms. Chiyumi Takeda, Ms. Kouko Motodate, and Toshiba Medical Systems for their excellent technical assistance.

## COMMENTS

### Background

Hepatitis C virus (HCV) has a high propensity to persist and cause chronic hepatitis, eventually leading to cirrhosis. Cirrhosis is an advanced stage of liver fibrosis that is accompanied by distortion of the hepatic vasculature. The evaluation of the hepatic vascular architecture is useful for assessing the HCV-related chronic liver disease (CLD) state, determining treatment strategies, and elucidating the mechanisms of disease progression. Therefore, the establishment of a noninvasive assessment tool of the hepatic vascular architecture is needed.

### Research frontiers

Recently, Toshiba Medical Systems has developed a new Doppler technique called superb microvascular imaging (SMI). SMI is an innovative ultrasound Doppler technology employing a unique algorithm that allows visualization of minute vessels with slow velocity. However, no reports to date have assessed hepatic vascular architecture in patients with HCV-related CLD using SMI.

## Innovations and breakthroughs

In this article, the authors validated that SMI allowed for the detailed delineation of the vascular architecture in CLD patients. Significant differences were found in the SMI pattern distribution and the fibrosis stage. Thus, SMI appears to be a reliable tool for noninvasively detecting significant fibrosis or cirrhosis in patients with HCV.

## Applications

The number of SMI signals in the region of interest (number of vascular trees: VT) can therefore be used as a noninvasive biological marker for the early detection and quantitative evaluation of distortion of the hepatic vasculature.

## Peer-review

The authors present valuable data from their research on the diagnosis of fibrosis using a new ultrasound Doppler technique called SMI in HCV patients.

## REFERENCES

- 1 **Krahn M**, Wong JB, Heathcote J, Scully L, Seeff L. Estimating the prognosis of hepatitis C patients infected by transfusion in Canada between 1986 and 1990. *Med Decis Making* 2004; **24**: 20-29 [PMID: 15005951 DOI: 10.1177/0272989X03261568]
- 2 **Serfaty L**, Aumaître H, Chazouillères O, Bonnard AM, Rosmorduc O, Poupon RE, Poupon R. Determinants of outcome of compensated hepatitis C virus-related cirrhosis. *Hepatology* 1998; **27**: 1435-1440 [PMID: 9581703 DOI: 10.1002/hep.510270535]
- 3 **Benvegnù L**, Gios M, Boccardo S, Alberti A. Natural history of compensated viral cirrhosis: a prospective study on the incidence and hierarchy of major complications. *Gut* 2004; **53**: 744-749 [PMID: 15082595 DOI: 10.1136/gut.2003.020263]
- 4 **Schuppan D**, Afdhal NH. Liver cirrhosis. *Lancet* 2008; **371**: 838-851 [PMID: 18328931 DOI: 10.1016/S0140-6736(08)60383-9]
- 5 **Wanless IR**, Wong F, Blendis LM, Greig P, Heathcote EJ, Levy G. Hepatic and portal vein thrombosis in cirrhosis: possible role in development of parenchymal extinction and portal hypertension. *Hepatology* 1995; **21**: 1238-1247 [PMID: 7737629 DOI: 10.1002/hep.1840210505]
- 6 **Wanless IR**, Shiota K. The pathogenesis of nonalcoholic steatohepatitis and other fatty liver diseases: a four-step model including the role of lipid release and hepatic venular obstruction in the progression to cirrhosis. *Semin Liver Dis* 2004; **24**: 99-106 [PMID: 15085490 DOI: 10.1055/s-2004-823104]
- 7 **Sato K**. [Angiographic study of the liver cirrhosis]. *Nihon Igaku Hoshasen Gakkai Zasshi* 1969; **28**: 1612-1628 [PMID: 5253941]
- 8 **Popper H**, Elias H, Petty DE. Vascular pattern of the cirrhotic liver. *Am J Clin Pathol* 1952; **22**: 717-729 [PMID: 14943688 DOI: 10.1093/ajcp/22.8.717]
- 9 **Hales MR**, Allan JS, Hall EM. Injection-corrosion studies of normal and cirrhotic livers. *Am J Pathol* 1959; **35**: 909-941 [PMID: 14398979]
- 10 **Baum S**, Roy R, Finkelstein AK, Blakemore WS. Clinical application of selective celiac and superior mesenteric arteriography. *Radiology* 1965; **84**: 279-295 [PMID: 14264589 DOI: 10.1148/84.2.279]
- 11 **Evans JA**. Specialized roentgen diagnostic technics in the investigation of abdominal disease. *Radiology* 1964; **82**: 579-594 [PMID: 14131663 DOI: 10.1148/82.4.579]
- 12 **Bosniak MA**, Phanumachinda P. Value of arteriography in the study of hepatic disease. *Am J Surg* 1966; **112**: 348-355 [PMID: 5920332 DOI: 10.1016/0002-9610(66)90202-9]
- 13 **Daly SM**, Leahy MJ. 'Go with the flow': a review of methods and advancements in blood flow imaging. *J Biophotonics* 2013; **6**: 217-255 [PMID: 22711377 DOI: 10.1002/jbio.201200071]
- 14 **Heimdal A**, Torp H. Ultrasound Doppler Measurements of Low Velocity Blood Flow: Limitations Due to Clutter Signals from Vibrating Muscles. *IEEE Trans Ultrason Ferroelectr Freq Control* 1997; **44**: 837-991 [DOI: 10.1109/58.655202]
- 15 **Ma Y**, Li G, Li J, Ren WD. The Diagnostic Value of Superb Microvascular Imaging (SMI) in Detecting Blood Flow Signals

- of Breast Lesions: A Preliminary Study Comparing SMI to Color Doppler Flow Imaging. *Medicine* (Baltimore) 2015; **94**: e1502 [PMID: 26356718 DOI: 10.1097/MD.0000000000001502]
- 16 **Machado P**, Segal S, Lyshchik A, Forsberg F. A Novel Microvascular Flow Technique: Initial Results in Thyroids. *Ultrasound Q* 2016; **32**: 67-74 [PMID: 25900162 DOI: 10.1097/RUQ.0000000000000156]
- 17 **Schneider CA**, Rasband WS, Eliceiri KW. NIH Image to ImageJ: 25 years of image analysis. *Nat Methods* 2012; **9**: 671-675 [PMID: 22930834 DOI: 10.1038/nmeth.2089]
- 18 **Bedossa P**, Poynard T. An algorithm for the grading of activity in chronic hepatitis C. The METAVIR Cooperative Study Group. *Hepatology* 1996; **24**: 289-293 [PMID: 8690394 DOI: 10.1002/hep.510240201]
- 19 **Pusztaszeri MP**, Seelentag W, Bosman FT. Immunohistochemical expression of endothelial markers CD31, CD34, von Willebrand factor, and Fli-1 in normal human tissues. *J Histochem Cytochem* 2006; **54**: 385-395 [PMID: 16234507 DOI: 10.1369/jhc.4A6514.2005]
- 20 **Poon RT**, Ng IO, Lau C, Yu WC, Yang ZF, Fan ST, Wong J. Tumor microvessel density as a predictor of recurrence after resection of hepatocellular carcinoma: a prospective study. *J Clin Oncol* 2002; **20**: 1775-1785 [PMID: 11919234 DOI: 10.1200/JCO.2002.07.089]
- 21 **Sugimoto K**, Shiraishi J, Moriyasu F, Ichimura S, Metoki R, Doi K. Analysis of intrahepatic vascular morphological changes of chronic liver disease for assessment of liver fibrosis stages by micro-flow imaging with contrast-enhanced ultrasound: preliminary experience. *Eur Radiol* 2010; **20**: 2749-2757 [PMID: 20571803 DOI: 10.1007/s00330-010-1852-1]
- 22 **Castéra L**, Nègre I, Samii K, Buffet C. Pain experienced during percutaneous liver biopsy. *Hepatology* 1999; **30**: 1529-1530 [PMID: 10610352 DOI: 10.1002/hep.510300624]
- 23 **Bravo AA**, Sheth SG, Chopra S. Liver biopsy. *N Engl J Med* 2001; **344**: 495-500 [PMID: 11172192 DOI: 10.1056/NEJM200102153440706]
- 24 **Friedrich-Rust M**, Wunder K, Kriener S, Sotoudeh F, Richter S, Bojunga J, Herrmann E, Poynard T, Dietrich CF, Vermehren J, Zeuzem S, Sarrazin C. Liver fibrosis in viral hepatitis: noninvasive assessment with acoustic radiation force impulse imaging versus transient elastography. *Radiology* 2009; **252**: 595-604 [PMID: 19703889 DOI: 10.1148/radiol.2523081928]
- 25 **Woo H**, Lee JY, Yoon JH, Kim W, Cho B, Choi BI. Comparison of the Reliability of Acoustic Radiation Force Impulse Imaging and Supersonic Shear Imaging in Measurement of Liver Stiffness. *Radiology* 2015; **277**: 881-886 [PMID: 26147680 DOI: 10.1148/radiol.2015141975]
- 26 **Zheng J**, Guo H, Zeng J, Huang Z, Zheng B, Ren J, Xu E, Li K, Zheng R. Two-dimensional shear-wave elastography and conventional US: the optimal evaluation of liver fibrosis and cirrhosis. *Radiology* 2015; **275**: 290-300 [PMID: 25575116 DOI: 10.1148/radiol.14140828]

**P- Reviewer:** Pellot-Barakat C, Ramanathan S **S- Editor:** Yu J  
**L- Editor:** Filipodia **E- Editor:** Zhang DN







Published by **Baishideng Publishing Group Inc**

8226 Regency Drive, Pleasanton, CA 94588, USA

Telephone: +1-925-223-8242

Fax: +1-925-223-8243

E-mail: [bpgoffice@wjgnet.com](mailto:bpgoffice@wjgnet.com)

Help Desk: <http://www.wjgnet.com/esps/helpdesk.aspx>

<http://www.wjgnet.com>



ISSN 1007-9327



9 771007 932045